JOURNAL OF MATERIALS SCIENCE **40** (2005) 423–428

Magnetic and dielectric properties of $Mg_{1+x}Mn_xFe_{2-2x}O_4$ ferrite system

A. A. PANDIT, A. R. SHITRE, D. R. SHENGULE, K. M. JADHAV*
Department of Physics, Dr. Babasaheb Ambedkar Marathwada University, Aurangabad - 431 004, India
E-mail: bamuaur@bom4.vsnl.net.in

Ferrites with the general formula $Mg_{1+x}Mn_xFe_{2-2x}O_4$ (where $x = 0.0$, 0.1, 0.2, 0.3, 0.4, 0.5, 0.6, 0.7, 0.8 and 0.9) were prepared by the standard ceramic technique and studied by means of X-ray diffraction, magnetization, a.c. susceptibility and dielectric constant measurements. The X-ray analysis confirmed the single-phase formation of the samples. The lattice parameter is found to increase up to $x = 0.3$ and thereafter it decreases as x increases. The cation distribution has been studied by X-ray analysis and magnetization. Magnetization results exhibit collinear ferrimagnetic structure for $x \leq 0.3$ and thereafter structure changes into non-collinear for $x > 0.3$. Curie temperature (T_C) obtained from a.c. susceptibility data decreases with increasing x. The dielectric constant (ε'), loss tangent (tan δ) show strong frequency dependence.

1. Introduction

Ferrites have been the subject of extensive study because of their wide range of applications from microwave to radio frequency and of their importance in understanding the theories of magnetism. They exhibit relatively high resistivity at carrier frequency, sufficiently low losses for microwave applications. These materials are extensively used in microwave devices, computer memory chips, magnetic recording media etc. [1].

Ferrites belonging to magnesium ferrite family having inherent rectangular hysteresis loop were first to be identified for the use in memory cores. The magnesium ferrite ($MgFe_2O_4$) is partially inverse ferrite [2] and it's degree of inversion depends upon heat treatment [3]. The interesting physical and chemical properties of ferrospinels arise from their ability to distribute the cations among the available tetrahedral (A) and octahedral [B] sites.

The knowledge of cation distribution and spin arrangement is essential to understand the magnetic properties of spinel ferrites. The addition of tetravalent ions and trivalent ions in ferrite influences the electrical and magnetic properties of the system [4–9]. The structural and magnetic properties of Mg ferrite with nonmagnetic substitution of divalent Zn^{2+}, Cd^{2+}, trivalent Al^{3+} and tetravalent Ti^{4+} have been investigated [10–13] by many workers. The substitution of magnetic ion such as Cr^{3+} in $MgFe_2O_4$ has been reported in the literature [14].

However, no reports are available in the literature on the magnetic and dielectric properties of magnetic Mn^{4+} substituted magnesium ferrite. Hence an attempt has been made to investigate the effect of magnetic Mn^{4+} substitution on the structural, magnetic and dielectric properties of $MgFe_2O_4$ by X-ray diffraction, magnetization, a.c. susceptibility and dielectric constant measurements. The present work reports the investigations carried out in the magnesium ferrite by simultaneously substituting Mg^{2+} in combination with a tetravalent magnetic Mn^{4+} ion.

2. Experimental

The samples of the general formula $Mg_{1+x}Mn_xFe_{2-2x}O_4$ were prepared by the standard ceramic technique for $0 \leq x \leq 0.9$ in steps of 0.1. The starting materials were analytical reagent grade oxides Fe_2O_3, MgO and MnO_2. These oxides were mixed in stoichiometric proportions, wet ground for four hours and presintered at 900°C for 12 h. In the final sintering process, the material was held at 1050°C for 24 h and slowly cooled to room temperature (2°C/min). The X-ray diffraction patterns for all the samples were recorded on Philips X-ray diffractometer (PW3710). The magnetization measurements were carried out using high field hysteresis loop technique [15] at 300 K. The a.c. susceptibility for the polycrystalline samples was measured using the double coil set up [16] operating at a frequency of 263 Hz and in r.m.s. field of 7Oe. The dielectric constant (ε') and loss tangent (tan δ) were measured in the frequency range 100 Hz to 1 MHz at room temperature using an HP 4284 LCR-Q meter.

*Author to whom all correspondence should be addressed.

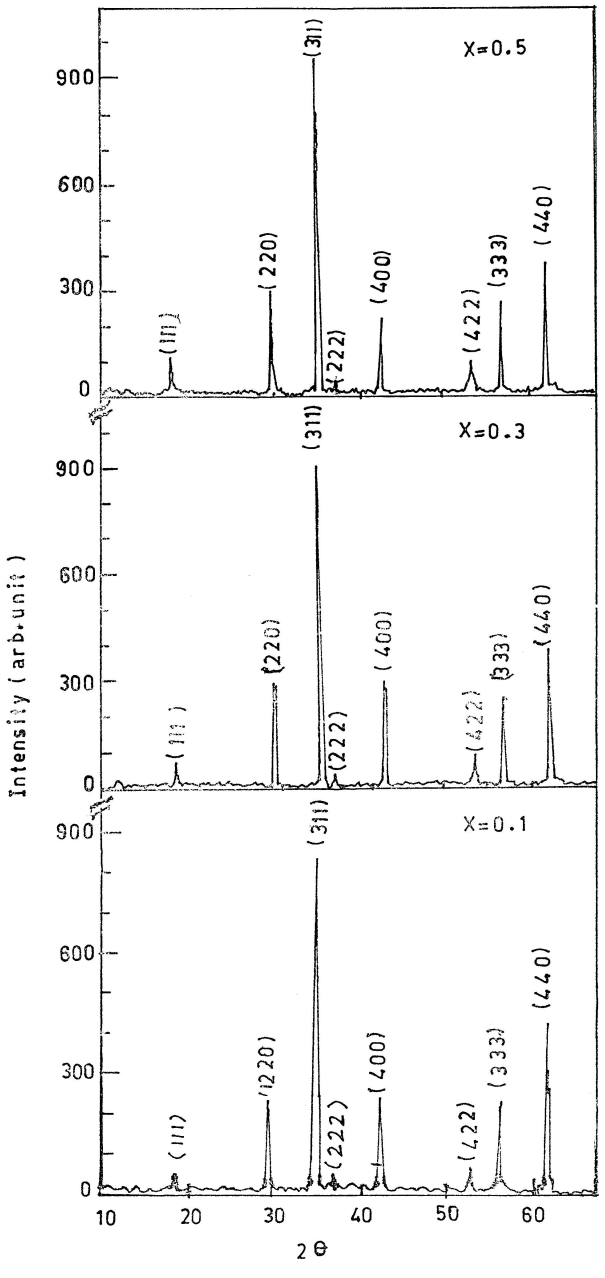

Figure 1 Typical X-ray diffraction patterns for $x = 0.1, 0.3$ and 0.5.

3. Results and discussion

X-ray diffraction patterns for all the ferrites under investigation have been obtained using Cu K_α radiations ($\lambda = 1.540$). Typical X-ray diffraction patterns for $x = 0.1$, 0.3 and 0.5 are shown in Fig. 1. Analysis of X-ray diffractograms reveals the formation of single-phase cubic spinels, showing well defined reflection of allowed planes. The lattice parameter of all the samples were calculated with an accuracy of ± 0.002 Å from XRD data.

The variation in lattice parameter with Mn^{4+} content is presented in Fig. 2. It can be seen from the Fig. 2 that the lattice parameter increases with x up to $x = 0.3$ and thereafter it decreases as x increases. This non-linear behaviour of lattice parameter (a) with composition x is attributed to the simultaneous replacement of Fe^{3+} ions (0.67 Å) by Mn^{4+}(0.52 Å) and Mg^{2+}(0.66 Å). The non-linear behaviour of 'a' with composition x may be due to the fact that the system under investigation is not

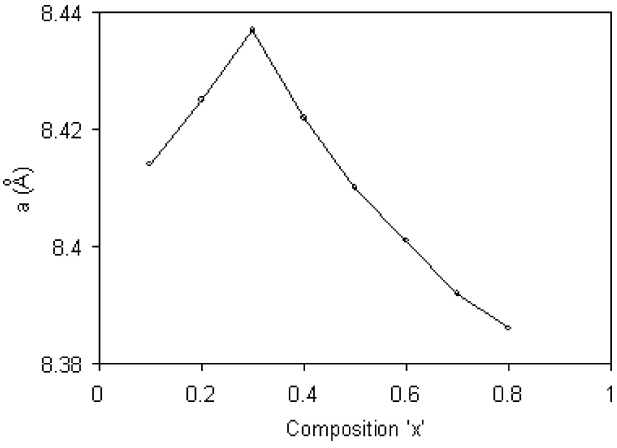

Figure 2 Variation of lattice constant 'a'(Å) with composition 'x'.

completely normal or inverse. Similar behaviour was reported by many workers [17, 18]. Initial increase in 'a' is an indication of the effect of addition of Mg^{2+} and Mn^{4+} ions. Further, decrease in 'a' for $x > 0.3$ is due to the replacement of larger Fe^{3+} ions by smaller Mg^{2+} and Mn^{4+} ions.

The X-ray density d_x is calculated according to the formula [19].

$$d_x = 8M/Na^3 \tag{1}$$

where M is the molecular weight, N is the Avogadro's number and 'a' is the lattice constant. The values of X-ray density are reported in Table I. It is seen that the X-ray density d_x decreases with increasing Mn content x.

The cation distribution in spinel ferrite was available from the study on the X-ray diffraction [20–22], Mössbauer effect [23] and magnetization methods [24]. According to Bertaut [25]. Weil Bertaut and Bochirol [26], the best information on cation distribution in spinel is achieved by comparing experimental and theoretical intensity ratios for reflections (220) and (440). According to Ohnishi and Teranishi [27] the intensity ratio of the planes $I_{(400)}/I_{(220)}$ and $I_{(422)}/I_{(400)}$ are considered to be sensitive to the cation distribution parameters. The distribution of cations among the available sites in spinel has been experimentally proved to an equilibrium function of temperature.

TABLE I Lattice constant (a) and X-ray density (d_x), for $Mg_{1+x}Mn_x$-$Fe_{2-2x}O_4$ system

Composition x	Lattice constant a (A)	X-ray density d_x (g/cm^3)
0.0	8.381	4.512
0.1	8.414	4.387
0.2	8.425	4.298
0.3	8.437	4.208
0.4	8.422	4.158
0.5	8.410	4.104
0.6	8.401	4.044
0.7	8.392	3.984
0.8	8.386	3.920
0.9	8.399	3.829

In the present method, the ratio of intensities of reflections due to the planes (220) and (400) has been chosen as a criterion to determine the cation distribution. The absorption and temperature factors are not taken into account in our calculations because these do not affect the relative intensity calculation for spinel at room temperature [28].

To determine cation distribution, it is necessary to calculate for each composition the I_{400}/I_{220}, I_{400}/I_{422} intensity ratios expected for given arrangement of the cations and compare them with the experimental values. For the calculation of the relative integrated intensity, 'I', of a given diffraction line from powder specimen, the following formula is valid [29].

$$I_{hkl} = |F|^2_{hkl} \cdot P \cdot L_P \tag{2}$$

where F is structure factor, P is multiplicity factor, L_P is Lorentz polarization factor.

For obtaining the cation distribution of $Mg_{1+x}Mn_xFe_{2-2x}O_4$ system, we have accepted the cation distribution of $MgFe_2O_4$ ($x = 0.0$) ferrite, which is represented by

$$(Mg_{0.07}Fe_{0.93})[Fe_{1.07}Mg_{0.93}] \tag{3}$$

and is close to the cation distribution given by other workers [30].

The structure factor, F is a function of oxygen parameter u, as well as distribution parameter y. The formulae for the structure factors for the planes (hkl) are taken from those reported by Furuhashi *et al.* [31]. The multiplicity factor and Lorentz polarization factor are taken from literature [19]. The ionic scattering factor reported in [32] are used for the calculation of the structure factor F.

The distribution of Mg^{2+}, Fe^{3+} and Mn^{4+} amongst octahedral [B] and tetrahedral (A) sites in the $Mg_{1+x}Mn_xFe_{2-2x}O_4$ was determined from the ratio of X-ray diffraction lines I_{400}/I_{220} and I_{400}/I_{422} (Table II).

Computerized calculation of intensity for the planes I_{400}/I_{220} I_{400}/I_{422} are performed for various values of distribution parameter y. The value of the distribution parameter y is reached by comparison of theoretical and experimental intensity ratios of (220) and (400), (400) and (422) planes. The value of y for which the theoretical and experimental ratios agree closely, is taken to be the correct one. The theoretical and experimental intensity ratios are compiled in Table II.

The electron exchange interaction ($Fe^{2+} \leftrightarrow Fe^{3+} + e^-$) results in a local displacements of electrons during the sintering process of ferrite. It has been reported that the jump length of electrons influences the physical properties of the ferrite system [33]. Electrons that are hopping between B and A sites are less probable compare to that between B and B sites, because the distance between two metal ions placed in B sites is smaller than that if they were placed one in B sites and the other in A sites [34, 35]. The jump length L on the octahedral site is determined from the following relation [36].

$$L = \frac{a\sqrt{2}}{4} \tag{4}$$

where a is the lattice parameter.

The variation of jump length L as a function of Mn^{4+} content x is shown in Fig. 3. It is observed from Fig. 3 that the jump length decreases with increase in Mn^{4+} content x.

The values of magneton number n_B (saturation magnetization per formula unit in Bohr magneton) at room temperature were obtained from hysteresis loop technique, by using the following relation [37].

$$n_B = \frac{\text{Molecular weight} \times \text{saturation magnetization}}{5585} \text{emu/g} \tag{5}$$

Table III gives the values of the saturation magnetization σ_s and the magneton number n_B. It is seen from Table III that the samples with $0.0 \leq x \leq 0.9$ show ferrimagnetic behaviour which decreases with increasing Mn^{4+} content. The variation of n_B with Mn^{4+} content x can be explained on the basis of the fact that non magnetic Mg^{2+} ions replaces the magnetic Fe^{3+} ions at tetrahedral sites A and due to the predominant inter sub-lattice A-B superexchange interaction, the net magnetic moment per formula unit is increased. The

TABLE II Cation distribution and intensity ratio for $Mg_{1+x}Mn_xFe_{2-2x}O_4$ system

		I_{220}/I_{400}		I_{422}/I_{400}	
Composition x	Cation distribution	Obs.	Cal.	Obs.	Cal.
0.0	$(Fe_{.93}Mg_{07})^A$ $[Fe_{1.07}Mg_{0.93}]^B$	1.175	2.032	0.404	0.688
0.1	$(Fe_{.85}Mg_{.15})^A$ $[Fe_{.95}Mn_{0.1}Mg_{0.95}]$	0.957	1.796	0.278	0.611
0.2	$(Fe_{.77}Mg_{023})^A$ $[Fe_{.83}Mn_{0.2}Mg_{0.97}]$	1.152	1.562	0.294	0.534
0.3	$(Fe_{.69}Mg_{031})^A$ $[Fe_{.71}Mn_{0.3}Mg_{0.99}]^B$	1.242	1.360	0.392	0.468
0.4	$(Fe_{.61}Mg_{.39})^A$ $[Fe_{.59}Mn_{0.4}Mg_{1.01}]^B$	1.133	1.181	0.223	0.408
0.5	$(Fe_{0.53}Mg_{.47})^A$ $[Fe_{0.47}Mn_{0.5}Mg_{1.03}]^B$	0.697	1.013	0.269	0.354
0.6	$(Fe_{0.45}Mg_{.55})^A$ $[Fe_{0.35}Mn_{0.6}Mg_{1.05}]^B$	0.966	0.877	0.237	0.307
0.7	$(Fe_{0.37}Mg_{.63})^A$ $[Fe_{0.23}Mn_{0.7}Mg_{1.07}]^B$	0.567	0.739	0.115	0.262
0.8	$(Fe_{0.29}Mg_{.71})^A$ $[Fe_{0.11}Mn_{0.8}Mg_{1.09}]^B$	0.714	0.616	0.108	0.220
0.9	$(Fe_{0.20}Mg_{.80})^A$ $[Mn_{0.9}Mg_{1.1}]^B$	0.363	0.500	0.060	0.179

TABLE III Saturation magnetization (σ_s), Magneton number (n_B), Yafet-Kittel angle (θ_{YK}) for $Mg_{1+x}Mn_xFe_{2-2x}O_4$ system

Composition x	Saturation magnetization σ_s (emu/g)	Magneton number n_B (μ_B)		Yafet-Kittel angle θ_{YK}	Curie temperature T_C (K)
		Obs.	Cal.		
0.0	17.99	0.644	0.7	0.0	690
0.1	27.00	0.812	0.8	0.0	670
0.2	27.70	0.960	0.9	0.0	650
0.3	29.03	0.997	1.0	0.0	645
0.4	28.58	0.957	1.1	15.08	640
0.5	27.81	0.726	1.2	22.18	635
0.6	19.82	0.629	1.3	35.80	630
0.7	16.30	0.517	1.4	43.24	625
0.8	12.38	0.386	1.5	51.51	620
0.9	8.08	0.247	1.7	62.49	610

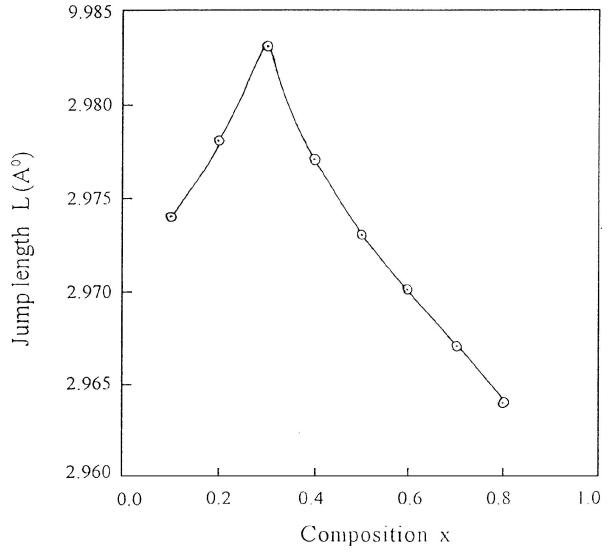

Figure 3 Variation of jump length L with Mn content x.

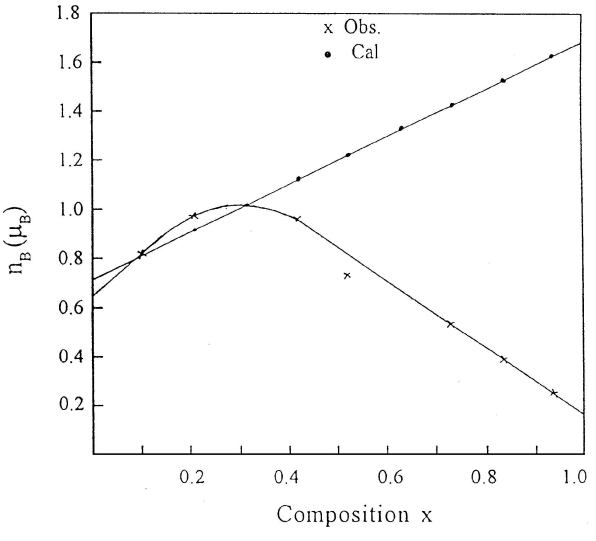

Figure 4 Variation of n_B with x.

variation of n_B with $x = 0.3$ is satisfactorily explained on the basis of Neel's two sub-lattices model of ferrimagnetism [38]. The decrease in n_B for $x > 0.3$ can be explained on the basis of Yafet-Kittel triangular type magnetic ordering of spins on the B sub-lattice.

According to Neel's two sub-lattice model of ferrimagnetism, the Neel's magnetic moment per formula unit in μ_B, n_B^N is expressed as,

$$n_B^N = M_B(x) - M_A(x) \tag{6}$$

where n_B^N is Neel magnetic moment per formula unit in μ_B, M_B and M_A are the B and A sub-lattice magnetic moment in μ_B. Since $MgFe_2O_4$ is a partially inverse spinel and Mn^{4+} ion has a tendency to occupy B-site, the cation distribution based on magnetization and X-ray intensity calculation has been given in Table II.

Compositional dependence of magneton number n_B in μ_B calculated from Neel's models for $x = 0.0$ to 0.9 using above equation and cation distribution is shown in Fig. 4. It can be seen from Fig. 4 that the calculated n_B^N values agree well with experimentally found values for $x = 0.0$ to 0.3, confirming a collinear magnetic structure. However for $0.3 < x < 0.9$ it clearly differs from the observed values indicating that significant canting exists on B-site, suggesting magnetic structure to be non-collinear for $x > 0.3$. The variation of n_B with x for $x > 0.3$ can be explained on the basis of Yafet-Kittel Model [39]. The Y-K angles were calculated by using the following formula,

$$n_B = M_B \cdot \cos\alpha_{yk} - M_A \tag{7}$$

and are given in Table III.

Thus, the change of spin ordering from collinear to non-collinear displays a strong influence on the variation of saturation magnetic moment per molecule as observed by magnetization (Fig. 4) with chemical composition.

The typical plots of a relative a.c. susceptibility $\chi T/\chi RT$ (RT = room temperature) against temperature (T) for $x = 0.2$, 0.4, 0.6 and 0.8 are shown in Fig. 5, which exhibits normal ferrimagnetic behaviour. A sharp peak near 500 K is observed for $x = 0.2$. As x increases the peak diminishes. Further it is observed that the susceptibility remains almost constant with temperature which is characteristic of multi domain (MD) particles. The Curie temperature determined from a.c. susceptibility measurements is shown in Fig. 6 as a function of x. It is observed from Fig. 6 that T_C decreases with the increase in x. The decrease in T_C is attributed to the fact that the A-B interaction decreases because of the replacement of Fe^{3+} ions by Mn^{4+} ions on the octahedral [B] sites and Mg^{2+} ions on the A sites.

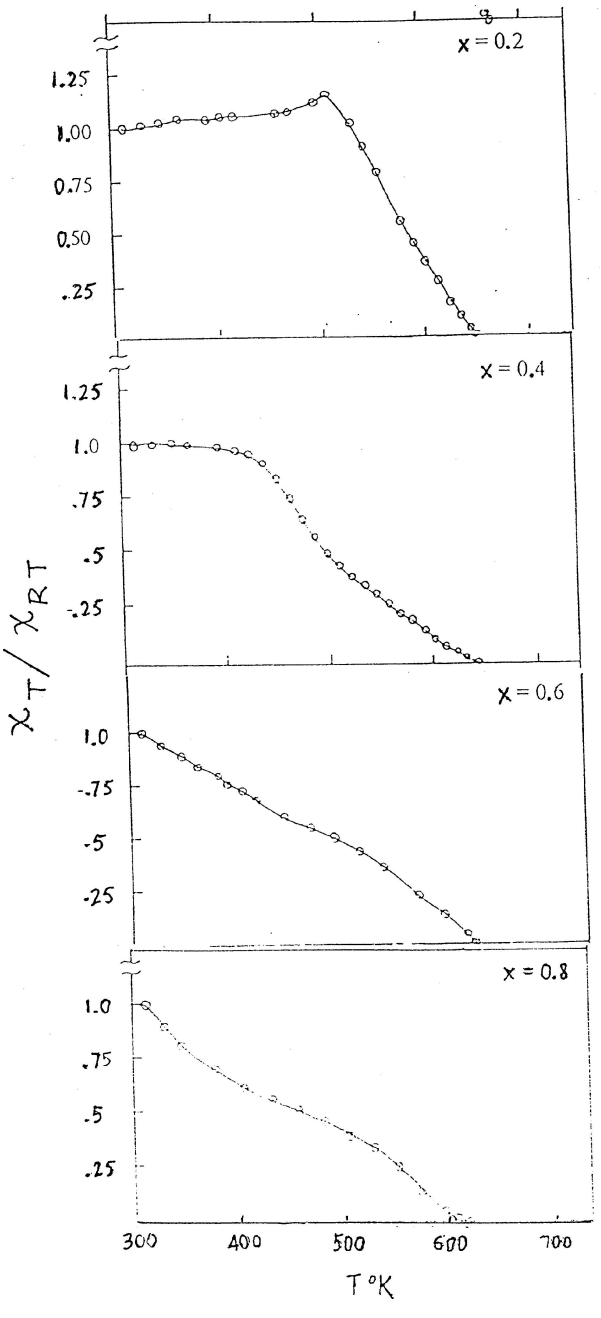

Figure 5 Thermal variation of a.c. susceptibility ($x = 0.2, 0.4, 0.6$ and 0.8).

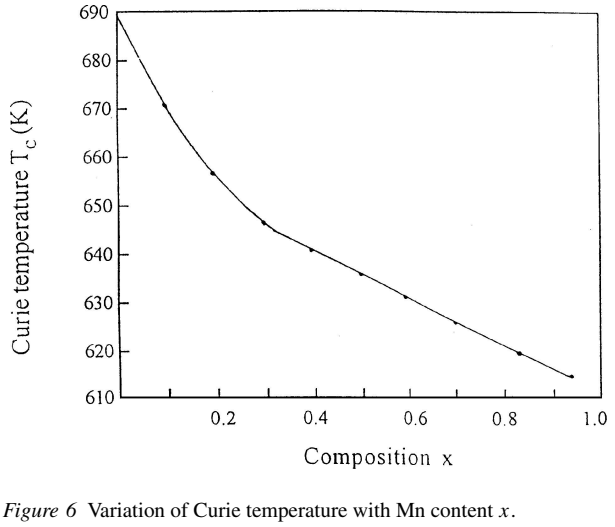

Figure 6 Variation of Curie temperature with Mn content x.

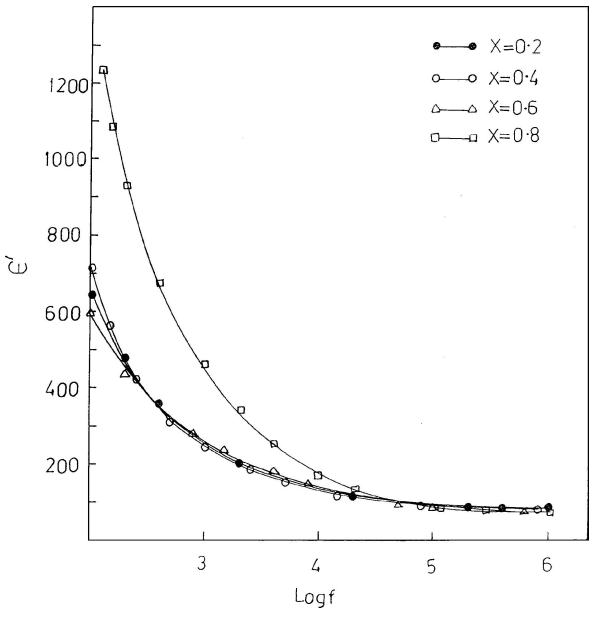

Figure 7 Variation of dielectric constant ε' with frequency for the samples with $x = 0.2, 0.4, 0.6$ and 0.8.

Since the polycrystalline ferrites are very good dielectric materials, the variation of dielectric constant (ε') and dielectric loss tangent ($\tan\delta$) is measured as a function of dopant concentration and frequency.

Fig. 7 shows the variation of dielectric constant with frequency measured at room temperature for typical samples $x = 0.2, 0.4, 0.6$ and 0.8. It can be seen from Fig. 7 that the dielectric constant (ε') decreases with the increase in frequency. The behaviour of frequency dependence of ε' for $Mg_{1+x}Mn_xFe_{2-2x}O_4$ is in very good agreement with the well known spinel ferrites [40, 41] for which ε' decreases continuously with increasing frequency range. A more dielectric dispersion is observed at low frequency region. This observed behaviour may be due to Maxwell-Wagner interfacial type of polarization [42, 43], which is in agreement with Koops phenomenological theory [44] by the electronic exchange

$$Fe^{3+} \leftrightarrow Fe^{2+} + e^{-1}$$

one obtains local displacement of electrons in the direction of the applied electric field. This displacement determines the polarization in ferrite. The decrease of polarization with increase of frequency may be due to the fact that beyond a certain frequency of the electric field, the electronic exchange between Fe^{2+} and Fe^{3+} cannot follow the alternating field, therefore the real part of dielectric constant decreases with increasing frequency.

The variation of dielectric loss tangent ($\tan\delta$) against log frequency at room temperature is depicted in Fig. 8 for $x = 0.2, 0.4, 0.6, 0.8$. It can be seen from Fig. 8 that all the samples show a normal dielectric behaviour with frequency. The parameter $\tan\delta$ decreases experimentally with the increase of frequency. A distinct maximum in $\tan\delta$ cannot be seen for any sample. The maximum in $\tan\delta$ occurs when the jump frequency of electron between Fe^{2+} and Fe^{3+} is equal to the frequency of the applied field [45].

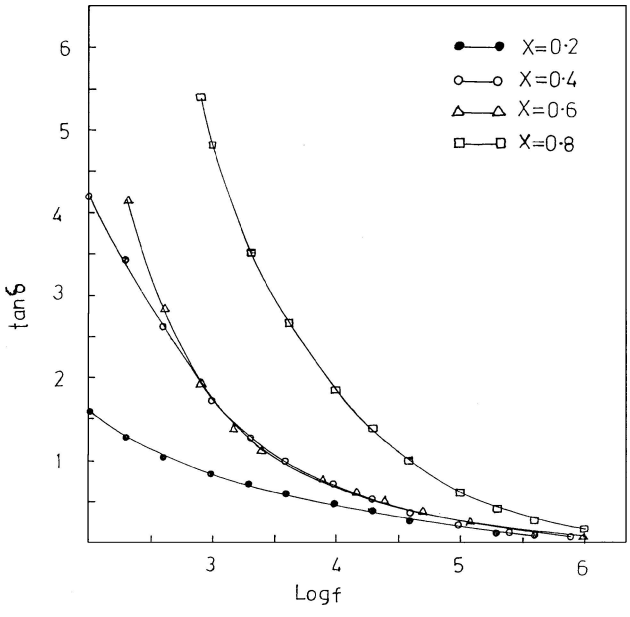

Figure 8 Variation of the dielectric loss tangent with frequency for the samples with $x = 0.2, 0.4, 0.6$ and 0.8.

4. Conclusion

The suggested cation distribution of the system $Mg_{1+x}Mn_xFe_{2-2x}O_4$ shows that Mn^{4+} occupy octahedral B site. Magnetization measurements exhibit Neel's collinear ferrimagnetic structure for $x = 0.0$ to 0.3 which is explained on the basis of Neel's model. The Curie temperature T_C obtained from a.c. susceptibility data decreases with the increase in Mn^{4+} content x. The dielectric constant ε' and loss tangent tan δ show strong frequency dependence.

Acknowledgements

One of the authors (A. A. Pandit) is grateful to the University Grant Commission, New Delhi for the award of fellowship under FDP program. The author K. M. Jadhav is thankful to U.G.C. (New Delhi) for granting major research project.

References

1. H. IGARASH and K. OKAZAKI, *J. Amer. Ceram. Soc.* **60** (1977) 51.
2. H. KNOCK and H. DANNHEIM, *Phys. Stat.* (a) (37) (1978) K135.
3. G. A. SAWATAKY, F. VANDER WOUDE and A. H. MORISH, *J. Appl. Phys.* **39** (1962) 1204.
4. H. H. JOSHI, R. B. JOTANIA and R.G. KULKARNI, *Solid State Commun.* **78** (1991) 539.
5. H. H. JOSHI and R. G. KULKARNI, *ibid.* **60** (1986) 67.
6. H. H. JOSHI, R. B. JOTANIA, G. KULKARNI and R. V. UPADHYAY, *Asian J. Phys.* **2** (1993) 88.
7. S. S. SHINDE, K. M. JADHAV, G. K. BICHILE, BIMAL S. TRIVEDI and R. G. KULKARNI, *Bull Mater Sci.* **21** (1998) 409.
8. R. K. PURI, M. SINGH and S. P. SUD, *J. Mater. Sci.* **29** (1994) 2182.
9. M. SINGH and S. P. SUD, *Mater. Sci. Engng.* B **83** (2001) 180.
10. R. G. KULKARNI and H. H. JOSHI, *Solid State Commun.* **49** (1985) 1005.
11. R. V. UPADHYAY and R. G. KULKARNI, *ibid.* **49** (1985) 69.
12. KUNAL B. MODI, V. T. THANKI and H. H. JOSHI, *Asian J. Phys.* **5** (1996) 461.
13. R. A. BRAND, H. GEORGES-GILBERT, J. HUBSCH and J. A. HELLER, *J. Phys. F: Mat. Phys., Mat. Sol.* **15** (1985) 1987.
14. A. D. BALAEV, O. A. BAYCSKOV and A. F. SAVITRKLL, *Phys. Stat. Sol.* (b) **152** (1989) 639.
15. C. RADHAKRISHNAMURTHY, S. D. LIKHITE and N. P. SASTRY, *Philos. Mag.* **23** (1971) 503.
16. C. RADHAKRISHNAMURTHY, S. D. LIKHITE and P. W. SAHASTRABUDHE, *Proc. Indian Acad. Sci.* **87A** (1978) 245.
17. D. C. KHAN, M. MISRA and A. R. DAS, *J. Appl. Phys.* **53** (1982) 2722.
18. S. J. SHUKLA, K. M. JADHAV and G. K. BICHILE, *Ind. J. Pure. Appl. Phys.* **39** (2001) 226.
19. B. D. CULLITY, "Elements of X-ray Diffraction" (Addison-Wesley Publishing, Reading, MA, 1956).
20. V. B. KAWADE, G. K. BICHILE and K. M. JADHAV, *Mater. Lett.* **42** (2000) 33.
21. D. S. BIRAJDAR, U. N. DEVATWAL and K. M. JADHAV, *J. Mater. Sci.* **37** (2002) 1443.
22. C. G. WHINFREY, D. W. ECKORT and A. TAABER, *J. Amer. Ceram. Soc.* **82** (1960) 1695.
23. N. N. JANI, B. S. TRIVEDI, H. H. JOSHI, G. K. BICHILE and R. G. KULKARNI, *Bull. Mater. Sci.* **21** (1998) 639.
24. S. R. SAWANT and R. N. PATIL, *Ind. J. Pure Appl. Phys.* **21** (1983) 145.
25. E. F. BERTAUT, *Compt. Rend.* **230** (1950) 213.
26. L. WEIL, E. F. BERTAUT and L. BOCHIROL, *J. Phys. Radium* **11** (1950) 208.
27. H. OHNISHI and T. TERANISHI, *J. Phys. Soc. Jpn.* **16** (1961) 36.
28. P. PORTA, F. S. STONE and R. G. TURNER, *J. Solid State Chem.* **11** (1974) 135.
29. M. G. BUERGER, "Crystal Structure Analysis" (Wiley, New York, 1960).
30. R. G. KULKARNI and H. H. JOSHI, *J. Solid State Chem.* **64** (1986) 141.
31. H. FURUHASHI, M. INAGAKI and S. NAKA, *J. Inorg. Nucl. Chem.* **35** (1973) 3009.
32. "International Tables for X-ray Crystallography" (Kynoch Press, Birmingham, 1968) Vol. III, p. 210.
33. M. EL. SAADAWY and M. M. BARAKAT, *J. Magn. Mag. Mat.* **213** (2000) 309.
34. K. STANDLEY, "Oxide Materials" (Clarendon, Oxford, 1972).
35. K. H. RAO, S. B. RAJU, K. AGGARWAI and K. G. MENDIRALLA, *J. Appl. Phys.* **52** (1981) 1376.
36. B. GILLOT and F. JEMMALI, *Phys. Stat. Sol.* (a) **76** (1983) 601.
37. S. A. PATIL, *Ind. J. Pure. Appl. Phys.* **21** (1983) 182.
38. L. NEEL, *C. R. Acad. Scin. Paris* **230** (1950) 375.
39. Y. YAFET and C. KITTEL, *Phys. Rev.* **87** (1952) 290.
40. A. R. SHITRE, V. B. KAWADE, G. K. BICHILE and K. M. JADHAV, *Mater. Lett.* **56** (2002) 188.
41. M. KORTZSCH, *Phys. Stat. Sol.* **6** (1964) 479.
42. J. C. MAXWELL, "Electricity and Magnetism" (Oxford University Press, Oxford Section) Vol. 1, p. 328.
43. K. W. WAGNER, *Ann. Phys. (Leipzig)* **40** (1913) 817.
44. C. G. KOOPS, *Phys. Rev.* **83** (1951) 1520.
45. J. SHOBHANADRI, *Phys. Status Solidi* **36** (1976) K133.

Received 17 June 2003
and accepted 3 June 2004